ISSN 1330-3651 (Print), ISSN 1848-6339 (Online)
https://doi.org/10.17559/TV-20230227000386
Original scientific paper

# Risk Assessment of Pressure Vessels by Using Fracture Mechanics and Advanced Ultrasonic Testing

Mirjana F. OPAČIĆ*, Aleksandar SEDMAK, Gordana BAKIĆ, Nenad MILOŠEVIĆ, Nikola MILOVANOVIĆ

**Abstract:** Risk assessment of cracked cylindrical pressure vessels for compressed air by using basic fracture mechanics and advanced methods of non-destructive testing (NDT), such as Phased Array Ultrasound (PAUT) and Time-of-Flight Diffraction (TOFD), is presented. Basic fracture mechanics equations are used to calculate the stress intensity factor, $K_I$, in the case of unacceptable defects found in the pressure vessel 970 in the Reversible Hydro Power Plant "Bajina Basta", and get the ratio $K_I/K_{Ic}$, according to the minimum measured values for fracture toughness for welded joints, as the typical zones where crack-like defects are found. The ratio $S_{net}/S_c$, where $S_{net}$ is the net stress in cross-section with a crack, and $S_c$ is the critical stress, is then evaluated to define the operating point in the Failure Assessment Diagramme (FAD), and thus, to estimate the likelihood of failure of the pressure vessel 970. In combination with estimated high consequence for the pressure vessel 970, the risk matrix was used, as a simple tool to assess the risk. In this paper the focus is on one aspect of this procedure, being the NDT role, since it is of utmost importance to use as precise as possible method for detected defects in welded joints. In this paper advanced ultrasound methods, PAUT and TOFD, are used to get precise image of defects in pressure vessel 970 welded joints, which were previously detected by conventional NDT methods. It is shown that the use of PAUT and TOFD is of utmost importance for decision making process in this case.

**Keywords:** PAUT; risk assessment; structural Integrity; TOFD

## 1 INTRODUCTION

To prevent failure, one can apply fracture mechanics equations to assess structural integrity of a component or construction, as applied for example in early Eighties, to solve problem of extremely large number of unacceptable defects in welded Alaska pipeline, [1]. More detailed explanation is provided from conceptual and historical perspective in [2-3], as well as in the case of large structures in [4]. The same concept was introduced and applied also in the case of life prediction and assessment, [5, 6]. The main idea was to avoid unnecessary and expensive repairs, if possible, which would also make more damage than be of any benefit in many cases. To do so, first it was up to researchers to prove that it is possible, and then, up to authorities to accept such an exemption from the rules, if reasonable arguments and conservative conclusions are provided. Here, the same thinking is used to present an engineering approach which can be applied in a simple way to get reliable and fast answer what to do in a situation when unacceptable defects are found in already operating equipment, which might be crucial in a plant (e.g. PV in RHE BB) and not available for repair or not suitable for it.

If one is looking for a simple engineering procedure to assess structural integrity of highly stressed thin component, starting point is stress-strain analysis. In the case of a simple geometry, like a cylindrical or spherical pressure vessel membrane plane stress state, analytical solutions are available, [7], whereas the finite element method is needed for more complex geometries, including cracks, and detailed stress analysis, [8-11]. In any case, for the further analysis probably the best option is the Failure Assessment Diagram (FAD), as shown in [12-13]. Furthermore, results of FAD can be used to estimate the likelihood of failure, which in combination with the consequence of failure enables the risk-based analysis, as introduced and applied recently, [14]. In this way engineers can provide all necessary information for managers, who are responsible for decision making process in respect to unacceptable defects.

Another important aspect here is the Non-Destructive Testing (NDT), especially if unacceptable defects are detected by conventional Ultrasonic Testing (UT), since their size might be over-conservatively estimated, due to some limitations of conventional UT, [15]. To overcome these limitations, new NDT techniques are recently introduced, such as the Phase Array (PAUT) and Time of Flight Diffraction (TOFD) [15-17].

The PAUT probe usually consists of numerous small elements (ultrasonic transducers; technical progress in on going 8, 16, 32 elements), and each of them is independently pulsed using the computer for timing calculation. By making the pulse delayed from each transducer in the timely manner, a pattern of constructive interference is set up, [15, 16]. To be more precise, with changing the progressive time delay the beam can be steered electronically, and the data from those beams can be put together to make a visual image that shows a slice through the object. In time-of-flight diffraction (TOFD) systems, a pair of ultrasonic probes are used, positioning them on opposite sides of a weld-joint in the area of interest, [15, 17]. In the part of welded joint without defect, the receiver probe is picking up signals from two waves: lateral wave one that travels along the surface and backwall reflection wave one that reflects off the far wall. When a discontinuity is present (such as crack), there is a diffraction of the ultrasonic sound wave from the top and bottom readings of the crack. If we use measured time of flight of the pulse, we can calculate the depth of the crack tips. Reliability of this method is higher than traditional radiographic, conventional manual UT and automated UT weld testing technique. One should notice that PAUT indicates the location of defect, whereas TOFD indicates length and depth of defect, making this combination optimal for sizing and positioning of a defect.

In this paper we consider welded joints in pressure vessels in Reversed Hydro Power Plant Bajina Basta (RHPP BB) in Serbia, where few defects, detected by conventional UT, were classified as unacceptable, and the most critical ones were analysed in the scope of structural

integrity assessment, [14]. Some of them were repaired, but most of them were left as they have not jeopardized vessel integrity. Although there were no mechanisms for their growth, these defects were monitored frequently just for the case. As it turned out, conventional UT detected small increase of a couple of defects, indicating a need to use additional, presumably more precise techniques of UT, [15]. Toward this end, a combination of PAUT and TOFD was used, as described in the following text.

## 2 APPLICATION OF BASIC FRACTURE MECHANICS EQUATIONS TO ASSESS STRUCTURAL INTEGRITY

Fracture mechanics equations can be applied in many different ways to assess structural integrity, depending on available data of material properties, geometry of a component or structure, including defects, and loading conditions. If the loading is static, there are two basic approaches, since material behaviour can be treated as linear elastic or as elastic-plastic. Therefore, either linear elastic or elastic plastic fracture mechanics equations are used.

Having in mind that welded joints are made of ductile materials, a more general, two-parameter approach which takes into account brittle failure and more plastic one. In the case of large pressure vessel, which is typically thin component under membrane plane stress state, the FAD can be used, as a simple engineering procedure, to assess its structural integrity. The FAD includes a limit curve, based on the modified strip-yield model for a through crack in an infinite plate, [18]:

$$\frac{K_{eff}}{K_I} = \frac{\sigma_C}{\sigma}\left[\frac{8}{\pi^2}\ln\sec\frac{\pi}{2}\frac{\sigma}{\sigma_C}\right]^{1/2} \tag{1}$$

where $K_I = \sigma\sqrt{\pi a}$, is the stress intensity factor, $K_{eff}$, its effective value, was introduced instead of $\delta$ ($K_{eff}^2 = \delta\sigma_Y E$), and $\sigma_Y$, Yield Stress (*YS*), was replaced by plastic collapse stress $\sigma_c$, value in between *YS* and tensile strength (*TS*), taken as an adequate yield criterion for structures like pressure vessels. Finally, $S_r = \sigma/\sigma_c$ and $K_r = K_I/K_{Ic}$ are defined, as convenient non-dimensional parameters. It was assumed thereby that $K_{eff}$ corresponds to the fracture toughness, so one gets the limit curve as follows, [18]:

$$K_r = S_r\left[\frac{8}{\pi^2}\ln\sec\left(S_r\frac{\pi}{2}\right)\right]^{1/2} \tag{2}$$

One should notice two extreme cases, structure made of a ductile material, failing due to plastic collapse at $S_r = 1$, and structure made of brittle material, failing at $K_r = 1$. In cases in-between these two extremes, plastic collapse and brittle fracture are mixed. If a point ($K_r$, $S_r$) is below the limit curve, a structure is safe, Fig. 1, [18].

One should notice that FAD provides more information about the structural integrity, than just YES/NO option, [14]. It is only natural to think about the likelihood of failure as being proportional to the position of a working point in FAD. Obviously, if point is close to 0, the likelihood is also close to 0, while for a point close to limit line it is certainly close to 1, as well. Thus, we adopt here definition of the Likelihood of Failure (*LoF*): $LoF = OA/OB$.

The risk-based assessment of cracked welded structures, like pressure vessels, can be performed by applying the risk matrix to estimate risk level according to the likelihood and consequence of failure, as shown in Tab. 1. Brief description of consequence categories is given in Tab. 2.

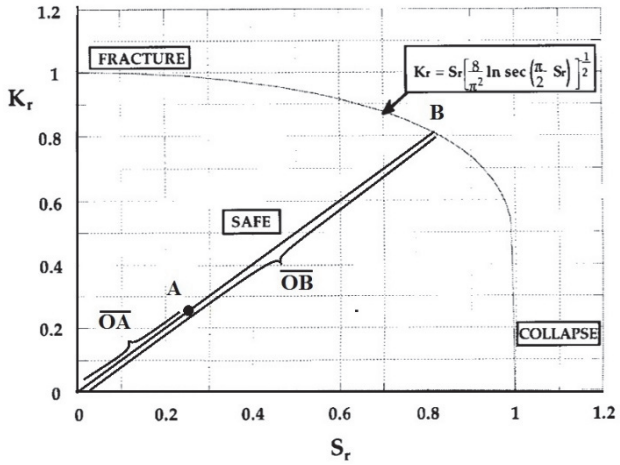


**Figure 1** Failure analysis diagram

**Table 1** Risk levels in relation to consequences and probability in risk matrix [14]

| Risk | | Consequence category | | | | |
|---|---|---|---|---|---|---|
| | | VL | L | M | H | VH |
| Likelihood category | VH | Medium | Medium high | Medium high | High | Very high |
| | H | Medium Low | Medium | Medium high | High | High |
| | M | Low | Medium | Medium | Medium high | Medium high |
| | L | Low | Low | Medium | Medium | Medium high |
| | VL | Very low | Very low | Low | Medium | Medium |

**Table 2** Consequence of failure categories [14]

| | A | B | C | D | E |
|---|---|---|---|---|---|
| Health (Long term visibility) | Warning issued No effect | Warning issued Possible impact | Temporary health problems, curable | Limited impact on public health, threat of chronical illness | Serious impact on public health, life threatening illness |
| Safety (Instatnt visibility) | No aid needed Work disruption | First aid needed No work disruption | Temporary work disability | Permanent work disability | Fatality (ies) |
| Enviromment | Negligible impact | Impact (e.g. spill) contained | Minor impact (e.g. spill) | On - site damage | Off - site damage Long term effect |
| Buisness / € | < 10 k€ | 10 - 100 k€ | 0.1 - 1 M€ | 1 - 1 M€ | > 10 M€ |
| Security | None | On - site (Local) | On - site (General) | Off site | Society threat |
| Image Loss | None | Minor | Bad publicity | Company issue | Political issue |
| Public disruption | None | Negligible | Minor | Small community | Large community |
| | Examples of CoF scales | | | | |

## 3 PRESSURE VESSELS IN RHE BB-INSPECTION IN 2019

Structural integrity of RHE BB pressure vessels has been analysed after unacceptable defects were found by Radiography in 1998 and confirmed by conventional UT later on. Conservative approach was applied, by using simple engineering tools, based on Failure Assessment diagram (FAD), as described in [14]. Stress intensity factors were calculated for an edge or central crack, representing crack-like defects in a cross-section, as the worst case option, and taking the minimum known value for the fracture toughness, according to previously done experiments on the same material, NIOVAL 50 (old generation HSLA steel), [19].

In the meantime, after 2019, additional UT (still conventional one) has been performed, indicating some changes of a few defects dimensions. Therefore, new analysis was performed to re-assess integrity of 3 pressure vessels with unacceptable defects as detected by conventional UT. One of these vessels, No. 970, is shown in Fig. 2, not only to illustrate the problem, but also to show original solution to the problem (stiffeners at the upper part), as will be explained later in more details. Just to mention, all PVs are of the same shape, with 3 circular and two longitudinal welded joints and somewhat different geometry, [14]. Inspection of pressure vessels was performed by NDT methods, first by visual testing standard EN ISO 5817: 2015, [20] and then by magnetic particle testing -standard EN ISO 23278 2020, [21], used for detection of surface and subsurface defects. Finally, Ultrasonic testing (UT) was used to detect internal defects, according to EN ISO 11666 2018, [22]. All welded joints (2 longitudinal and 3 circumferential, Fig. 2) were tested by 100% UT by using USM 36XL Kraut Kramer device.

After the final conventional UT testing of all vessels, 3 of them have been chosen for more detailed analysis, PV 977 with defect 2.5, PV 971 defect 1.1 and 970 defect 5.6. One should notice that there are no residual stresses in these PVs due to Post-Weld-Heat-Treatment (PWHT), while the material properties are as follows:

- Fracture toughness $K_{Ic}$ for the weld metal is taken as 1580 MPa$\sqrt{}$mm in all cases, being the minimum value (in HAZ), as shown in [19].
- Collapse stress $\sigma_c$ taken as the mid-value between $YS$ = 500 MPa, $TS$ = 650 MPa.

Pressure vessel 970 defect 5.6:

Basic data needed for risk-based assessment:

- thickness $t$ = 50 mm, mean diameter $D$ = 2150 mm.
- Pressure $p$ = 8.1 MPa.

**Figure 2** PV 970 in RHEBB

The largest defect found, using conventional UT testing, was defect 5.6, length $2c$ = 75 mm, depth $a$ = 20 mm, positioned along the thickness from 18 to 38 mm, in a longitudinal joint.

To calculate the stress intensity factor for central surface crack ($c$ = 75 mm, $2a$ = 20 mm) one can use the following expression:

$K_I = Y(a/W, a/c)\,(pR/t)\sqrt{\pi a} = 1{,}1(174)\sqrt{10\pi} =$

$=1075$ MPa$\sqrt{}$mm,

where the geometry factor $Y(a/W) = 1.10$ is evaluated for the following data: $a/W = 20/50 = 0.4$, $a/c = 20/75 = 0.27$, [23]. Now one can calculate the ratio $K_I/K_{Ic} = 0.72$, being the $Y$ coordinate of the point in the FAD.

To get the $X$ coordinate, one should calculate the ratio between net cross-section stress, $\sigma_n$, and collapse stress $\sigma_c$:

$S_R = \sigma_n/\sigma_F = 167.7 \times 1.74/575 = 0.49$

Coordinates for defect 5.6 in FAD are (0.49; 0.72), positioning the point in the safe region, Fig. 3, with likelihood of failure ($LoF$) 0.77.

Pressure Vessel 971 - defect 1.1:

Basic data needed for risk-based assessment:

- thickness $t$ = 50 mm, mean diameter $D$ = 2150 mm.
- Pressure $p$ = 8.1 MPa.

The largest defect found in the vessel 971, using conventional UT testing was defect 1.1, length $2c$ = 180 mm, depth $a$ = 32 mm (18 - 50 mm along the thickness), circular seam with the bottom lid.

Stress intensity factor for an edge surface defect with dimensions $2c = 180$ mm, $a = 32$ mm, can be calculated as:
$K_I = Y(a/t, a/c)\,(pR/2t)\sqrt{\pi a} = 1{,}83(87)\sqrt{32\pi} = \quad = 1520$ MPa$\sqrt{\text{mm}}$
where $Y$ (0.64, 0.35) = 1.83, [23], so one gets the ratio $K_R = K_I/K_{Ic} = 0.96$. Ratio between net cross-section stress and collaps stress in this case is:
$S_R = \sigma_n/\sigma_F = 87 \cdot 2.78/575 = 242/575 = 0.42$

Therefore, coordinates are (0,42; 0.96), Fig. 3, positioning the point in FAD very close to the limit line, with $LoF = 0.99$.

Pressure Vessel 977 - defect 2.5:

Basic data needed for risk-based assessment:

- thickness $t = 42$ mm, mean diameter $D = 1958$ mm.
- Pressure $p = 7.8$ MPa.

The largest defect found in the vessel 971, using conventional UT testing was defect 2.5. length $2c = 170$ mm, depth $a = 14$ mm (28 - 42 mm along the thickness of the mid-circular joint).

The stress intensity factor for edge surface defect ($2c = 170$ mm, $a = 14$ mm), is calculated as:
$K_I = Y(a/W)\,(pR/2t)\sqrt{\pi a}$,
where $Y(a/W) = 1.82$, [17, 18], for $a/t = 0.33$, $a/c = 0.16$, resulting $K_I = 1050$ MPa$\sqrt{\text{mm}}$ and $K_I/K_{Ic} = 0.66$. Ratio between net cross-section stress and collaps stress is:
$S_R = \sigma_n/\sigma_F = 136/575 = 0.24$,
where $\sigma_n = 90.9/0.67 = 136$ MPa. The point with coordinates (0.24; 0.66) is in FAD safe area, Fig. 3, with $LoF = 0.71$.These three points are presented in the FAD, Fig. 3, indicating different levels of $LoF$.

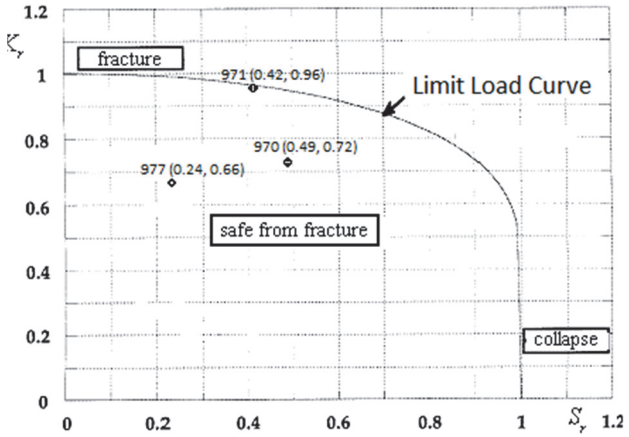


**Figure 3** Points in FAD for pressure vessels 970, 971 and 977

## 4 RISK-BASED ASSESSMENT

In this paper risk level is determined according to the likelihood, evaluated for the most critical defects (5.6 in PV 970, 1.1 in PV 971 and 2.5 in PV 977) and the consequence, which is evaluated as the highest one, after careful consideration of the failure scenario. The risk matrix is shown in Tab. 3, indicating very high risk for PV 971, as well as high risk for PV 970 and 977.

**Table 3** Risk matrix for pressure vessel 970, 971 and 978

| Risk | | Consequence category | | | | |
|---|---|---|---|---|---|---|
| | | VL | L | M | H | VH |
| Likelihood category | VH | | | | | 971 defect 1.1 |
| | H | | | | | 977 defect 2.5<br>970 defect 5.6 |
| | M | | | | | |
| | L | | | | | 971 "new" defect* |
| | VL | | | | | |

*"new" defect refers to the result of additional NDT by using advanced UT

In all 3 cases, actions were needed, taking into account specific conditions, as follows:

- Defect 2.5: it was decided to remove it by grinding and then to repair PV 977 by welding.
- Defect 5.6: repair welding was not an option, so a special design solution in the form of a stiffener was suggested and executed for PV 970.
- Defect 1.1: since neither repair welding nor the special design solution was an option, and additional NDT from the inner side of the vessel (VT, MT) did not reveal the presence of this defect, it was decided to use more advanced UT for additional testing of PV 971.

## 5 PRESSURE VESSEL 971 INSPECTION IN 2022

Having in mind this analysis, advanced UT techniques, PAUT and TOFD, were recently applied as the optimal combination to define in a more precise way dimensions and location of defect 1.1. Testing was performed using the Sonatest Veo + 32/128 device with Sonatest UT Studio + software. Transversal waves were used, sound velocity of 3240 m/s, impulse-echo method, along with Sector scanning and test amplification 45,5 dB. Contrary to the conventional UT Technique, two indications were found instead of a single one: The first one with length 53.1 mm, and depth 16.7 mm (extending from 12.4 to 29.1 mm); the second one with length 18.8 mm, and depth 3.5 mm, from 46.9 to 50.4 mm, Fig. 4.

All necessary details of the UT testing by combination of PAUT and TOFD advanced techniques are presented in Fig. 4, where the first defect is denoted by AN1, and the second one by AN2. Upper screenshot shows TOFD results, whereas the lower one shows PAUT.

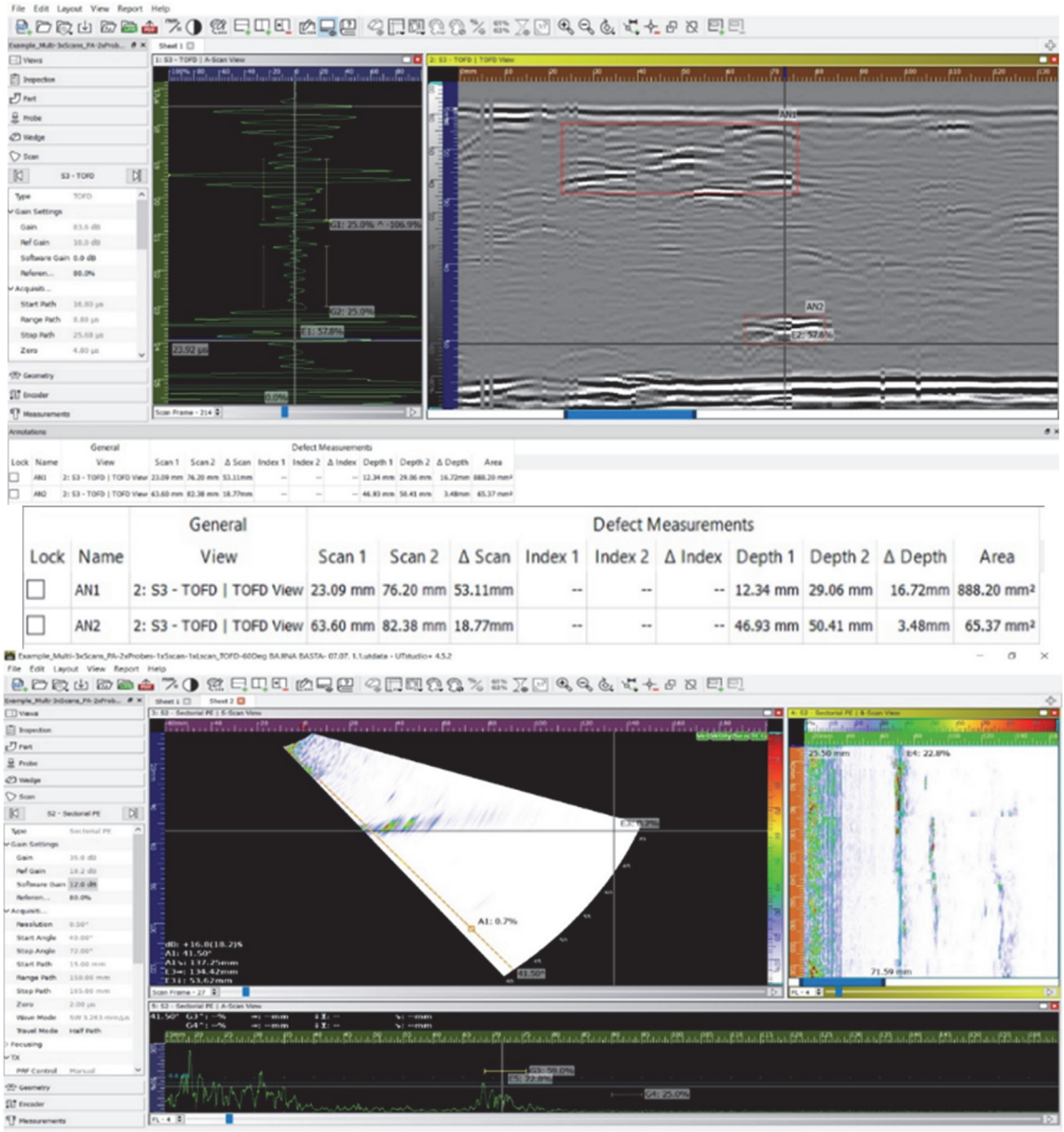

| Lock | Name | General View | Scan 1 | Scan 2 | Δ Scan | Index 1 | Index 2 | Δ Index | Depth 1 | Depth 2 | Δ Depth | Area |
|---|---|---|---|---|---|---|---|---|---|---|---|---|
| | AN1 | 2: S3 - TOFD \| TOFD View | 23.09 mm | 76.20 mm | 53.11mm | -- | -- | -- | 12.34 mm | 29.06 mm | 16.72mm | 888.20 mm² |
| | AN2 | 2: S3 - TOFD \| TOFD View | 63.60 mm | 82.38 mm | 18.77mm | -- | -- | -- | 46.93 mm | 50.41 mm | 3.48mm | 65.37 mm² |

**Figure 4** Indications and results of PAUT and TOFD testing [15]

Also taking into account the material thickness was found to be 55 mm (not 50 mm as found by conventional UT), even though both indications are still unacceptable, it is all too clear that the risk of failure is significantly lower than predicted by using measurements of conventional UT. Results obtained by PAUT and TOFD are also in accordance with the fact that no crack was found on the inner side of the vessel. Finally, it should be mentioned that these two indications are not in the same plane, so they are not likely to merge. Based on this, risk-based re-assessment for defect 1.1 was performed as follows.

For the internal crack with $2c$ = 53.1 mm and $2a$ = 16.7 mm, the stress intensity factor was re-calculated as follows:

$K_I = Y(a/t,\ a/c)\ (pR/2t)\sqrt{\pi a} = 1{,}01(87)\sqrt{8.35\pi} =$ = 450 MPa$\sqrt{\text{mm}}$, leading to the ratio $K_R = K_I/K_{Ic} = 0.28$.

Ratio between net cross-section stress and collapse stress in now:

$S_R = \sigma_n/\sigma_F = 87 \cdot 1.5/575 = 130.5/575 = 0.23$

Points coordinated in the Fracture Assessment Diagram (FAD) are now (0,23; 0.28), leading to the level of fracture likelihood 0.3, and the risk level tothe medium, instead of very high, as shown in Tab. 2.

## 7 DISCUSSION AND CONCLUSIONS

Risk-based assessment can be rather complex and complicated procedure, but also relatively simple if FAD is taken as an engineering tool to evaluate likelihood of failure and if at the same time descriptive evaluation of consequence of failure is sufficient. In other words, if it is obvious what is the consequence category of a concrete problem, as is the case analysed here and if time is limited when equipment like PV in RHPP is available for testing and eventual repair or replacement, there is an additional argument in favour of using simple and efficient method for risk-based assessment.

When compared to other UT techniques, PAUT has few important advantages, since it can be conducted much faster, in repeatable manner and can make multiple scans at once, [24]. Also, in combination with TOFD it can detect precisely dimensions and location of a defect. Both techniques are followed by encoder, all data can be recorded

and saved for future analysis and proof. PAUT also has some advantages considering other UT techniques, since there is no, dead zone" as it is the case with any other available UT method".

Based on the results presented in this paper one can conclude that PAUT and TOFD are of utmost importance for more precise detection of defects than conventional UT can do, especially in the case of inner defects, not reaching the outer surfaces. One should think of these two techniques as the best combination to get precise dimensions and location of a defects. Therefore, they are crucial for reliable assessment of structural integrity of critical components, such as pressure vessels, as well as for precise evaluation of failure risk, providing sound basis for decision making process.

**Acknowledgements**

Authors acknowledge the support of the Ministry of Science, Technological Development and Innovation of the Republic of Serbia (Contract No. 451-03-47/2023-01/200105 and 451-03-47/2023-01/200213).

## 8 REFERENCES

[1] Reed, R. P., Kasen, M. B., McHenry, H. I., & Fortunko, C. M. (1983). Fitness-for-Service Criteria for Pipeline Girth Weld Quality. https://doi.org/10.6028/NBS.IR.83-1695

[2] Toribio, J. (2020). Towards a new concept of structural integrity. *Procedia Structural Integrity, 26*, 354-359. https://doi.org/10.1016/j.prostr.2020.06.045

[3] Francois, D. (1996). From the European Group on Fracture to the European Structural Integrity Society. *Materials Science*, *32*(5), 531-536. https://doi.org/10.1007/BF02539062

[4] Fekete, T. (2022). The Fundaments of Structural Integrity of Large-Scale Pressure Systems. *Procedia Structural Integrity*, *37*, 779-787. https://doi.org/10.1016/j.prostr.2022.02.009

[5] Tonković, Z., Somolanji, M., & Stojšić, J. (2009). Life prediction of damaged PE 80 gas pipes. *Tehnički vjesnik*, *16*(3), 33-37.

[6] Drobne, M., Vuherer, T., Samardžić, I., & Glodež, S. (2014). Fatigue crack growth and fracture mechanics analysis of a working roll surface layer material. *Metalurgija*, *53*(4), 481-484.

[7] Qananah, H. R., Petrović, R., Banaszek, A., Anđelković, M., Cvejić, R., Đorđević, N., & Milovanović, N. (2022).Stress state optimisation of vertical atmospheric large-volume tanks. *Structural integrity and Life*, *22*(2), 247-252.

[8] Milovanović, A. M., Martić, I., Trumbulović, L., Diković, L., & Drndarević, B. (2021). Finite element analysis of spherical storage tank stress state. *Structural Integrity and Life*, *21*(3), 273-278.

[9] Sedmak, A. (2018). Computational fracture mechanics: An overview from early efforts to recent achievements. *Fatigue & Fracture of Engineering Materials & Structures*, *41*(12), 2438-2474. https://doi.org/10.1111/ffe.12912

[10] Kirin, S., Sedmak, A., Zaidi, R., Grbović, A., & Šarkočević, Ž. (2020). Comparison of experimental, numerical and analytical risk assessment of oil drilling rig welded pipe based on fracture mechanics parameters. *Engineering Failure Analysis*, *114*, 104600. https://doi.org/10.1016/j.engfailanal.2020.104600

[11] Zhou, R., Gu, X., Bi, S., & Wang, J. (2022). Finite element analysis of the failure of high-strength steel pipelines containing group corrosion defects. *Engineering Failure Analysis*, *136*, 106203. https://doi.org/10.1016/j.engfailanal.2022.106203

[12] Sedmak, A., Zaidi, R., Vujičić, B., Šarkočević, Ž., Kirin, S., Đukić, M., & Bakić, G. (2022). Corrosion effects on structural integrity and life of oil rig drill pipes: Original scientific paper. *Hemijska industrija* (*Chemical Industry*), *76*(3), 167-177. https://doi.org/10.2298/HEMIND220222014S

[13] Sedmak, A., Arsić, M., Šarkoćević, Ž., Medjo, B., Rakin, M., Arsić, D., & Lazić, V. (2020). Remaining strength of API J55 steel casing pipes damaged by corrosion. *International Journal of Pressure Vessels and Piping*, *188*, 104230. https://doi.org/10.1016/j.ijpvp.2020.104230

[14] Golubović, T., Sedmak, A., Spasojević Brkić, V., Kirin, S., & Rakonjac, I. (2018). Novel risk based assessment of pressure vessels integrity. *Tehnički vjesnik*, *25*(3), 803-807. https://doi.org/10.17559/TV-20170829144636

[15] Opačić, M., Sedmak, A., Bakić, G., Milošević, N., & Milovanovic, N. (2022). Application of advanced NDT methods to assess structural integrity of pressure vessel welded joints. *Procedia Structural Integrity*, *42*, 1185-1189. https://doi.org/10.1016/j.prostr.2022.12.151

[16] Raj, B. & Jayakumar, T. (1997). NDE methodologies for characterisation of defects, stresses and microstructures in pressure vessels and pipes. *International journal of pressure vessels and piping*, *73*(2), 133-146. https://doi.org/10.1016/S0308-0161(97)00042-2

[17] Pugalendhi, P. & Veerarju, D. (2013). Use of Phased Array Ultrasonic Testing (PAUT) & Time of Flight Diffraction (TOFD) in Lieu of Radiography Testing on ASME U Stamp Pressure Vessel fabrication Projects. *Singapore International NDT Conference & Exhibiton.*

[18] Anderson, T. (2004). Fracture Mechanics Fundamentals and Applications, *CRC Press*. https://doi.org/10.1201/9781315370293

[19] Gerić, K. (1997). *Crack initiation and growth in high strength steel welded joints*. Doctoral Thesis, University of Belgrade.

[20] International Organization for Standardization. (2015). *Welding Quality levels for imperfections*. (EN ISO 5817:2015)

[21] International Organization for Standardization. (2020). *Non-destructive testing of welds*. (EN ISO 23278: 2020)

[22] International Organization for Standardization. (2018). *Ultrasonic testing Acceptance levels*. (EN ISO 11666: 2018)

[23] Newman Jr., J. C. & Raju, I. S. (1981). An empirical stress-intensity factor equation for the surface crack. *Engineering fracture mechanics*, *15*(1-2), 185-192. https://doi.org/10.1016/0013-7944(81)90116-8

[24] Kurz, J. H., Jüngert, A., Dugan, S., Dobmann, G., & Boller, C. (2013). Reliability considerations of NDT by probability of detection (POD) determination using ultrasound phased array. *Engineering failure analysis*, *35*, 609-617. https://doi.org/10.1016/j.engfailanal.2013.06.008

**Contact information:**

**Mirjana F. OPAČIĆ**, PhD Sc. student
(Corresponding author)
Innovation Center of Faculty of Mechanical Engineering,
Kraljice Marije 16, 11120 Belgrade, Republic of Serbia
E-mail: mopacic@mas.bg.ac.rs

**Aleksandar SEDMAK**, Professor Emeritus
University of Belgrade, Faculty of Mechanical Engineering,
Kraljice Marije 16, 11120 Belgrade, Republic of Serbia
E-mail: asedmak@mas.bg.ac.rs

**Gordana BAKIĆ**, Professor
University of Belgrade, Faculty of Mechanical Engineering,
Kraljice Marije 16, 11120 Belgrade, Republic of Serbia
E-mail: gbakic@mas.bg.ac.rs

**Nenad MILOŠEVIĆ**, Assistant Professor
University of Belgrade, Faculty of Mechanical Engineering,
Kraljice Marije 16, 11120 Belgrade, Republic of Serbia
E-mail: nmilosevic@mas.bg.ac.rs

**Nikola MILANOVIĆ**, PhD
Innovation Center of Faculty of Mechanical Engineering,
Kraljice Marije 16, 11120 Belgrade, Serbia
E-mail: nmilovanovic@mas.bg.ac.rs